RESEARCH ARTICLE

Molecular Dynamics and FEM Modeling of Composites Having High Thermal Conductivity

Sumit Sharma*, Pramod Kumar, Ajay Kumar Diwakar

Department of Mechanical Engineering, Dr. B R Ambedkar National Institute of Technology Jalandhar, Punjab, India

*Corresponding author: E-mail: sharmas@nitj.ac.in; Tel.: (+91) 8146871758

DOI: 10.5185/amlett.2020.091557

Nowadays there is a requirement of material that has high thermal conductivity as well as suitable electric insulating properties. Such materials are required in industries where thermal management is desirable but electrical conductivity is not required, such as substrates for electronic components and solar panels. In this study, the multi-scale modeling of epoxy (bisphenol-A) reinforced alumina composite has been performed using BIOVIA Materials Studio and Abaqus. Modeling has been done for varying volume fraction (V_f) of alumina. The properties predicted are the thermal conductivity and Young's modulus. Heat transfer analysis has been done using Abaqus/Explicit. It was found that the thermal conductivity first increased till V_f = 20% and then decreased. When the concentration of alumina was increased further after V_f = 20%, the orientation of alumina particles changed from being in-plane to random, resulting in a fall in the values of thermal conductivity. In the silicon/insulator plate system, there was found to be an accumulation of heat resulting in a decrease in temperature on the bottom surface of the insulator plate. Thus, more time was taken for the heat to conduct through this system. Whereas, when the heat was transferred through the system of silicon/composite plate, no accumulation of heat in the system was observed.

Introduction

The performance and life of electronic devices are greatly affected by the phenomena of heat transfer. Since this is the age of miniaturization of electronic devices there is an urgent need for materials having high thermal conductivity as well as excellent electrical insulation. Polymers have been used extensively for electronic packaging applications (Chen *et al.* (2016), Lin *et al.* (2014)) but these have poor thermal conductivity values which lie between 0.1-0.5 W/mK (Han and Fina (2011)). Because of such low thermal conductivity, polymers have been rarely used for applications concerning heat transfer. However, polymers reinforced with thermally conductive materials such as aluminium oxide (Al_2O_3), aluminium nitride (AlN), graphene, and carbon nanotube (CNT) have gained significant importance because of the high value of heat transfer.

Xu *et al.* (2001) studied the polymer matrix composites that were thermally conductive but electrically insulating. For developing such composites, the materials used were AlN, SiN, and polyvinylidene fluoride (PVDF) and epoxy whiskers or particles as the matrix. With PVDF, the thermal conductivity was increased to 11.5 W/mK. To find the thermal conductivity of aligned multi-walled CNT-polymer composite, a theoretical model was developed by Bagchi and Nomura (2006). It was found that most of the heat was carried by the outer tube resulting in lower values of thermal. Yu *et al.* (2009) used molecular dynamics (MD) and sequential scale bridging methods to investigate the effect of Al_2O_3 nanoparticles on the properties of EPON862–TETA polymer-based composites. Kozako *et al.* (2010) discussed the ways to improve the thermal conductivity, relative permittivity, and dielectric strength of alumina particle reinforced epoxy composites. The thermal conductivity and dielectric strength of the composite materials were found to improve with the addition of hybrid fillers.

Sharma *et al.* (2017) studied the effect of the geometry of nano-filler on the thermal conductivity and Young's modulus of single-layer graphene sheets–copper and carbon nanotube–copper composites. Single-layer graphene sheets–Cu composites exhibited a higher rate of increase in thermal conductivity as well as Young's modulus with an increase in vol. %, in comparison to the carbon nanotube–Cu composites. Nakayama *et al.* (2016) suggested a method to improve the thermal conductivity of polymer nanocomposites at low values of filler volume fraction (15 vol.%) by making the use of hexagonal boron nitride (BN) nanosheets. Flexible nanocomposite films with linear densely packed BN structures (LDPBNs) showed higher values of thermal conductivity as well as electrical resistivity.

Lei *et al.* (2016) fabricated thermally conductive carbon filler (S-filler) reinforced polypropylene (blended with alumina) (PP/Al_2O_3) composites. Upon addition of 15 wt.% S-filler, both the DC electrical resistivity as well as the thermal conductivity were found to improve. Yang *et al.* (2018) fabricated thermally conductive and electrically insulating layered SiR/GNPs/BN composites using a combination of carbon-based and ceramic-based filler. The composites exhibited high values of thermal conductivity (8.45 W/m.K) and were found to be highly insulating. Fu *et al.* (2019) used the melt blending process to prepare nylon 6 (PA6)/graphene nanoplatelets (GNPs)

composites. These were then coated with hexagonal boron nitride (h-BN) powder and were finally hot pressed. The thermal conductivity was found to improve by approximately ten times at 18.82 vol.% fillers. The composites also showed a high value of electrical insulation. Jazani *et al.* (2016) prepared epoxy-based adhesives reinforced with silica and alumina fillers (20, 40, and 60 phr) and were successfully applied for lap-joint bonding of carbon fiber composite with steel. Lap shear test suggested a considerable improvement of about 12% and 20%, compared to unfilled epoxy/hardener systems, for composites containing 60 phr of alumina and silica, respectively. Saeb *et al.* (2018) prepared silicone/clay nanocomposite coatings and their curing state was discussed by defining a puzzle for silicone/clay systems, which received cure characteristics of nanocomposites including T_P and ΔH together with those of blank silicone rubber and gives T^* and ΔH^* dimensionless indexes as the output of puzzle, which made it possible to study the network formation in such complicated systems under the influence of clay incorporation, concentration, and surface chemistry. Saeb *et al.* (2015) produced highly curable epoxy/multi-walled carbon nanotube (MWCNT) nanocomposites by introducing primary and secondary amino groups onto the surface of carbon nanotubes. The calculated heats of cure assigned to the systems containing amino-MWCNTs were higher than that of those with unmodified MWCNTs and even higher with respect to unfilled epoxy/anhydride composites. Duan *et al.* (2011) examined a method for enhancing the heat transfer from a given surface adaptively by using a shape memory alloy (SMA). The SMA was attached to the cooling sidewalls. The analysis showed that the temperature of the hot sidewalls could be kept around a temperature that the material could bear even though the heat flux change from the scramjet combustion was 2 MW/m^2. Xu *et al.* (2020) studied experimentally the effects of copper foam and ultrasonic vibration on the melting process of low-melting gallium in a rectangular vessel. The effective thermal conductivity, heating wall temperature, most melting duration, and total melting duration during the gallium's melting process were examined for various heating powers. It was found that a portion of the gallium remained solid in the corners of the vessel in the late melting stage, and melting the remaining solid portion accounted for approximately 28% of the total melting duration of the pure gallium. Yilmazoglu *et al.* (2019) analyzed an electronic driver unit of an HVAC (heating, ventilating, and air conditioning) system operated in a dusty environment within an enclosure. The effects of fin spacing, fin thickness, base thickness, and heat sink positions were simulated. According to the performance improvement results, the temperatures of the triacs were decreased by 10.1% and 13.2%, respectively.

Aghdam and Ansari (2019) developed a new micromechanical formulation based on a unit cell model to predict the effective thermal conductivities of CNT-shape memory polymer (SMP) nanocomposites. The effects of volume fraction, diameter, cross-section shape, arrangement type, and waviness factors of CNTs as well as interfacial thermal resistance on the axial and transverse thermal conductivities of aligned CNT-reinforced SMP nanocomposites were extensively investigated. The results showed that the alignment of CNTs into the SMP nanocomposites along the thermal loading could be an efficient way to dissipate the heat. Mahmoodi *et al.* (2018) established a hierarchical approach to investigate the thermal conducting behavior of micro filler (in the form of a particle, short and long fiber)/nanoparticle-reinforced polymer hybrid nanocomposites. The results were provided for two types of hybrid nanocomposites, including carbon micro filler/silica (SiO_2) nanoparticle-reinforced epoxy and glass micro filler/SiO_2 nanoparticle-reinforced epoxy systems. It was found that the transverse thermal conducting behavior of general fibrous composites was significantly affected by adding the nanoparticles. Jamali *et al.* (2018) analyzed the thermal conductivities of CNT-coated fiber reinforced nanocomposites. The transverse thermal conductivity was found to increase with the CNT coating however, the longitudinal thermal conductivity of carbon fiber-reinforced hybrid nanocomposites was not affected by the CNTs coating. Mahmoodi *et al.* (2018) predicted the thermal conductivities of general CNT reinforced polymer nanocomposites using the effective medium approach. The effects of volume fraction, diameter, the non-straight shape of CNTs, interfacial thermal resistance, and temperature were investigated on the nanocomposite overall heat transfer behavior. The results emphasized that the consideration of the proper waviness and 3D random orientation of CNTs together with the interfacial thermal resistance into the analysis was essential for a more realistic prediction.

The computational tools have developed rapidly in the last decade. This has helped MD simulation to become an important tool for the investigation of various chemical and physical phenomena. MD simulation has been used widely for predicting the mechanical and thermal properties of a variety of materials. This has resulted in the development of new materials with unique properties without following the cumbersome path of experiments. MD simulations have reduced the cost and time associated with the experimental procedure. MD simulations are thus nowadays widely accepted by the research community. Though MD simulations have been used for the prediction of properties of polymer-based composites but to the best of the authors' knowledge, there is a dearth of research on materials having high thermal conductivity and low electrical conductivity. Nowadays there is a requirement of material that has high thermal conductivity as well as suitable electric insulating properties. Such materials are required in industries where thermal management is desirable but electrical conductivity is not required, such as substrates for electronic components and solar panels. The objective of this study is to develop a novel material that fulfills the above-stated criteria. In this study, the

multi-scale modeling of epoxy reinforced alumina composite has been performed using BIOVIA Materials Studio and Abaqus. The modeling has been done for the various volume fraction of alumina. Heat transfer analysis has been done using Abaqus/Explicit. The properties predicted are the thermal conductivity and Young's modulus.

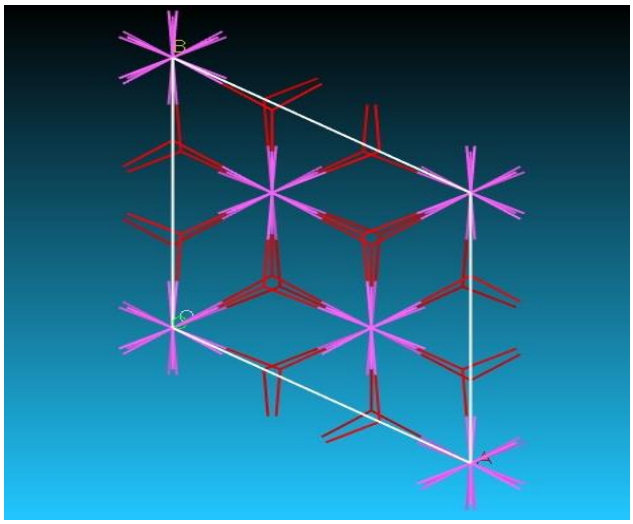

Fig. 1. Unit cell of pure alumina (Al_2O_3).

Computational technique

Firstly, the structure of pure Alumina was modeled using BIOVIA Materials Studio 7.0 (Dassault Systemes BIOVIA (2017)). **Fig. 1** shows the unit cell of pure Alumina. Then, using the 'build' option a nanocluster was modeled having a radius of 5 Å and having 64 atoms as shown in **Fig. 2**. A monomer of epoxy (bisphenol A), as shown in **Fig. 3**, was built by using the "Build repeat unit" tool of BIOVIA Materials Studio 7.0 (Dassault Systemes BIOVIA (2017)). **Fig. 4** shows a single chain of the epoxy polymer consisting of 10 repeat units of epoxy. Condensed phase optimized molecular potential for atomistic simulation studies (COMPASS) (Sun (1998)), a most common force field, was used for describing both inter and intra-molecular atomic interactions. The density of commercially available epoxy was taken as 1.25 g/cm^3 (Schulte *et al.* (2003)). The bisphenol-A epoxy was then packed around the alumina particle using the "Amorphous cell" module of BIOVIA Materials Studio 7.0. One such packing has been shown in **Fig. 5**. The size of the simulation cell was taken as 14.00 Å X 14.00 Å X 14.00 Å, which provided the alumina volume fraction of 20 %. Stability was provided to the structure by minimizing the energy of the system. In this study, the energy was minimized using the "conjugate gradient algorithm" (Yu *et al.* (2009)). The system was considered to be optimized when the change in energy between subsequent steps was less than 1X10^{-4} kcal/mol. A total of 50000 iteration steps were performed during the task of geometry optimization.

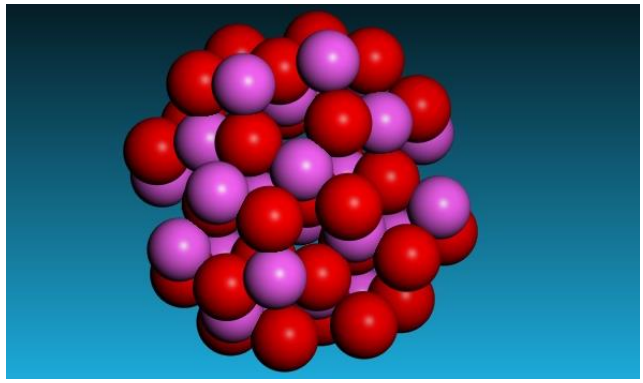

Fig. 2. Alumina nanocluster having radius of 5 Å and containing 64 atoms.

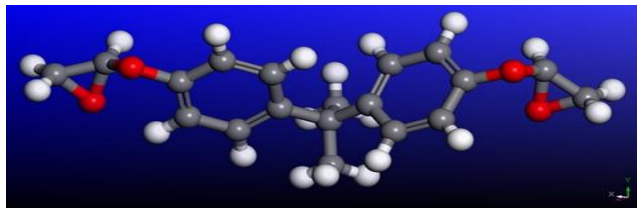

Fig. 3. Epoxy (bis-phenol A) monomer.

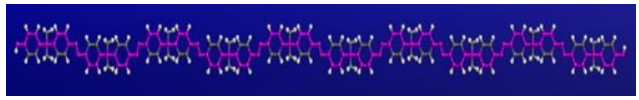

Fig. 4. A chain of the epoxy polymer consisting of 10 repeat units of epoxy.

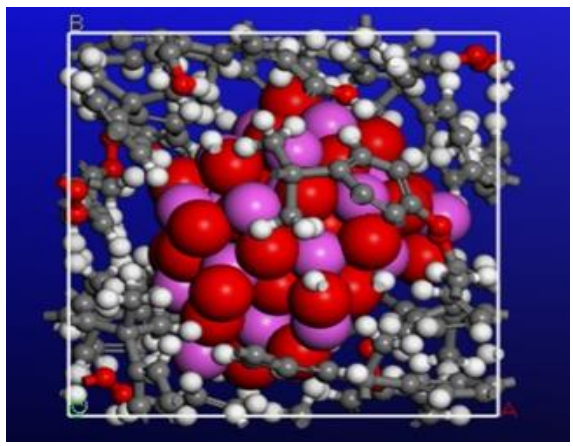

Fig. 5. Amorphous cell packed alumina with epoxy having a total 376 atoms.

Dynamics run was performed to compress the system, obtain the proper density, and to reduce the residual stresses. The first step of dynamics was performed using the constant number of atoms, volume, and temperature (NVT) ensemble at 300K. The total simulation time provided was 500ps with the time step of 1fs. This was followed by another dynamics run for 900ps with time-step 0.2fs and using the constant number of atoms, pressure, and temperature (NPT) ensemble with a pressure of 1atm to equilibrate the system and to obtain the final trajectory that has been fully equilibrated. To obtain the mechanical properties, a stress-strain script was written using the Perl script module of BIOVIA Materials Studio.

The script could be found in the supplementary data provided with this work. Similarly, for finding the thermal conductivity a script was written using the same module. The details of the script could be found in another work by the authors (Sharma (2019)). The mechanical and thermal properties obtained from MD were then used as input for Abaqus. The methodology used in Abaqus Explicit (Dassault Systèmes Simulia Corp, USA (2017)) has been shown in **Fig. 6**. Both Abaqus Standard and Abaqus Explicit provide coupled temperature displacement analysis procedures, but the algorithms used by each program differ considerably. In Abaqus/Standard the heat transfer equations are integrated using a backward-difference scheme, and the coupled system is solved using Newton's method. These problems can be transient or steady-state and linear or nonlinear. In Abaqus/Explicit the heat transfer equations are integrated using an explicit forward-difference time integration rule, and the mechanical solution response is obtained using an explicit central-difference integration rule. Fully coupled thermal-stress analysis in Abaqus/Explicit is always transient. Cavity radiation effects cannot be included in a fully coupled thermal-stress analysis. In this study, Abaqus Explicit has been used.

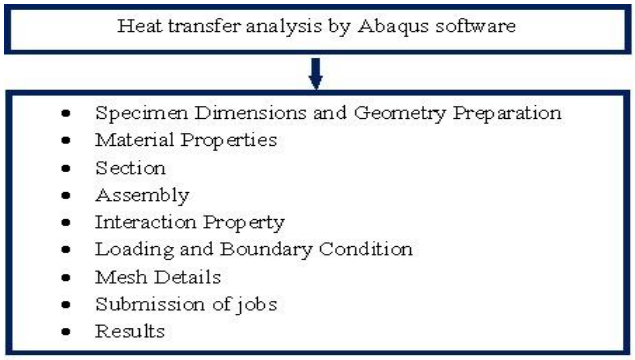

Fig. 6. Methodology used in Abaqus.

There were two systems for which heat transfer analysis was performed. The first system was (i) Silicon and insulator plates and the second system consisted of (ii) Silicon and composite (epoxy and alumina) plates. Both systems were modeled using the 'Parts' module of Abaqus. The dimensions of both the specimen were kept the same as shown in **Table 1**.

Table 1. Specimen dimensions (Tyagi et al. (2012)).

Dimensions (in mm)	
Width of the plate (b)	150
Thickness of the silicon plate (h)	0.3
Thickness of the insulator/composite plate (h)	0.6
Length of the beam (L)	150

Table 2. Material properties for the two systems.

Property	Silicon	Epoxy	Insulator	Alumina	Epoxy-Alumina composite (at 20% V_f)
Thermal conductivity (W/m.K)	130 (Khelifa et al. (2016))	0.24 (Khelifa et al. (2016))	0.03 (Khelifa et al. (2016))	38-42 (Khelifa et al. (2016))	1.90 (from MD)

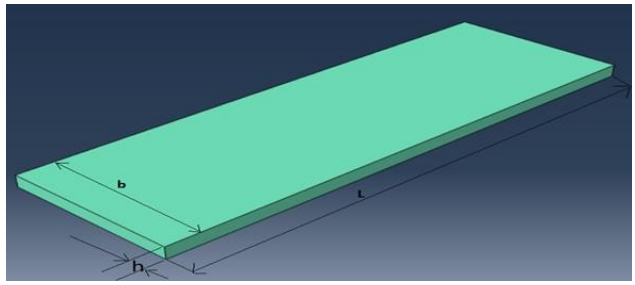

Fig. 7. Dimensions of plates used for heat transfer analysis.

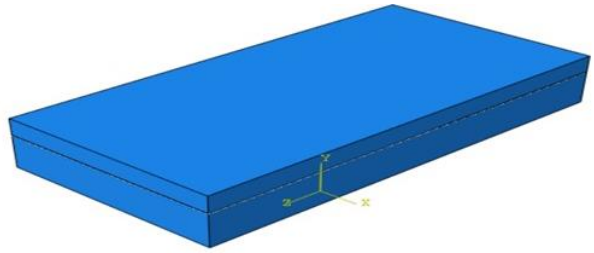

Fig. 8. Assembly of plates.

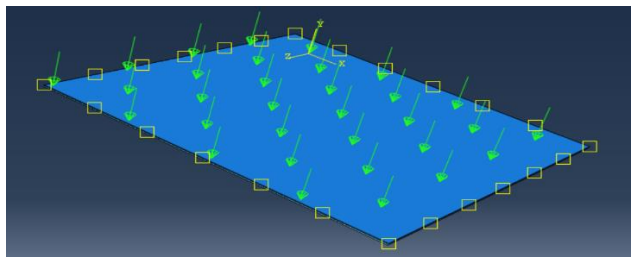

Fig. 9. Heat flux and temperature defined as input parameters for the plate system.

Also, **Fig. 7** shows the dimensions of the plates modeled in Abaqus/Explicit. The two plates were then combined to give the final model, as shown in **Fig. 8**. Such a system could be found in hybrid photovoltaic/thermal (PV/T) collector systems. **Fig. 8** shows the system of plates in which the silicon plate lies on the upper side having thickness 0.3 mm and the lower side was taken as an insulator or composite material plate having a thickness of 0.6 mm. At the lower surface, the convective heat transfer coefficient of air was given. Heat flux and temperature were given on the upper surface of assembly and at the lower surface, convective heat transfer arrangement was made as shown in **Fig. 9**. The heat transfer coefficient for air varied as 10-100 W/m K, so in this analysis 50 was chosen as the average value and the sink temperature was set as the room temperature. After making the assembly, constraint heat flux of 1000 W/mK was given along with an upper plate temperature of 343 K to get the temperature at the lower surface. The loading and boundary conditions have been shown in **Table 3**. The meshing details of the system have been shown in **Table 4** and **Fig. 10**. The hex mesh generally works better (i.e., more accurate) for wall-bounded flows since orthogonal grids in the wall-normal direction can be maintained. This is a consequence of the better accuracy of the hex elements since the angle between faces can be kept close to 90-degrees. The DC3D8 element was chosen along with

the meshing type as 'hex'. The size of each element was taken as 0.002 mm and 6750 elements were used for modeling the complete system. There were 8192 nodes in the system shown in **Fig. 10**.

Table 3. Loading and boundary conditions.

Heat flux(W/m K)	Temperature (K)	Film coefficient	Sink temperature
1000	343	50	296.15

Table 4. Mesh details.

Element Type	Element Shape	Element	Nodes	Element Size
DC3D8	Hex	6750	8192	0.002 mm

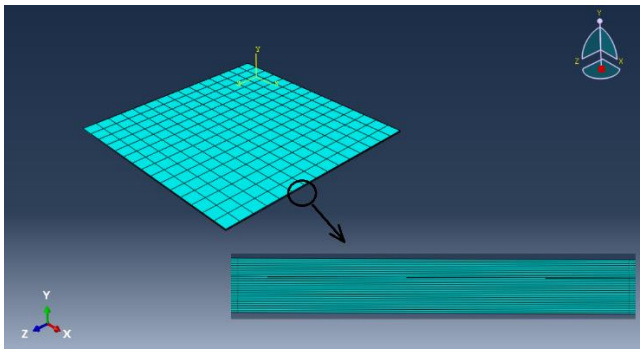

Fig. 10. Meshed model of combined plates having 6750 elements and 8192 nodes.

Results and discussion

In this section, the results of heat transfer analysis of the two systems: (i) composite (epoxy and alumina) and silicon and (ii) silicon and insulator, have been discussed. The composite material was formed with different volume fractions of alumina with epoxy as a matrix. The thermal conductivity of the epoxy-alumina composite was obtained using MD simulations. The thermal conductivity of silicon and insulator were known (Tyagi *et al.* (2012)) and further heat transfer analysis was performed using Abaqus/Explicit software. Using the scripts developed by the authors in another work (Sharma (2019)), the thermal conductivity of epoxy-alumina composite at alumina volume fractions (V_f) of 15%, 20%, and 25% were found to be 1.63, 1.90 and 0.77 W/mK respectively. It was found that at alumina V_f = 21%, the thermal conductivity of epoxy-alumina composite was found to be 1.5 W/mK. Thus, it could be inferred that as V_f of alumina particles was increased, the thermal conductivity of the composite also increased until V_f = 20%. After this value, the thermal conductivity was found to decrease. This could be attributed to the fact that at low values of V_f, the alumina particles were lying in the plane of heat conduction thus increasing the thermal conductivity. When the concentration of alumina was increased further after V_f = 20%, the orientation of alumina particles changed from being in-plane to random, resulting in a fall in the values of thermal conductivity (Mai *et al.* (2019)). The Young's moduli of epoxy-alumina composite obtained through the stress-strain script for V_f = 20% have been shown in **Table 5**. Young's moduli of the epoxy-alumina composite at V_f = 20% were 17.77, 5.56, and 7.06 GPa at applied stress of 50, 60, and 70 GPa respectively. The results obtained for thermal conductivity have been compared with previous studies as shown in **Table 6**. From Table 6, it could be inferred that the epoxy (bisphenol A)/alumina composite could be useful for thermal management applications in nanoelectronics and solar panels.

Table 5. Young's modulus of epoxy-alumina composite obtained through stress strain script for V_f = 20%.

S. No.	Input stress (GPa)	Measured stress (GPa)	Strain	Strain Modulus (GPa)
1.	50	4.94548359	0.27830269	17.77016066
2.	60	6.89007421	1.23742134	5.56809067
3.	70	33.25977507	4.70671113	7.06645769

Table 6. Comparison of thermal conductivity of epoxy-alumina composite obtained from present study with other researchers.

	Material used	Thermal conductivity (W/mK)
Present study	Epoxy-alumina (at V_f =20%)	1.90
Nakayama et al. (2016)	Polysiloxane/BN-nanosheet (at V_f =15%)	1.56
Lei et al. (2016)	CNT/polypropylene (alumina) composite (at 15 wt.% of CNT)	0.68

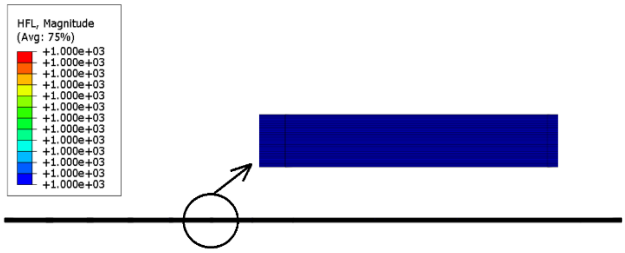

Fig. 11. Heat flux of 1000 W/m^2 passed through plates.

Fig. 11 shows the variation of heat flux through the thickness of the plates when a flux of 1000 W/m^2 was passed through plates. From **Fig. 11**, it was observed that there was no change in the heat flux transferred through the plates along the thickness and was found to be independent of the type of material of the plate. The heat flux remained constant for both the systems as shown in **Fig. 12**. It was noticed that the thermal conductivity of silicon plate (130 W/m K) was enough to transfer heat but the insulator plate used below it had very low thermal conductivity (0.03 W/m K). This resulted in a large temperature difference for the given heat flux. It could be seen from **Fig. 13** that the nodal temperature on the top surface was 343 K and at the thickness of 0.9 mm (bottom surface) it decreased to 319.6 K. This resulted in a temperature difference of 23.4 K. Because of the low thermal conductivity of the insulating material, accumulation of heat could take place in this system resulting in a decrease in temperature on another surface. Thus, more time would be taken for the heat to transfer through this system.

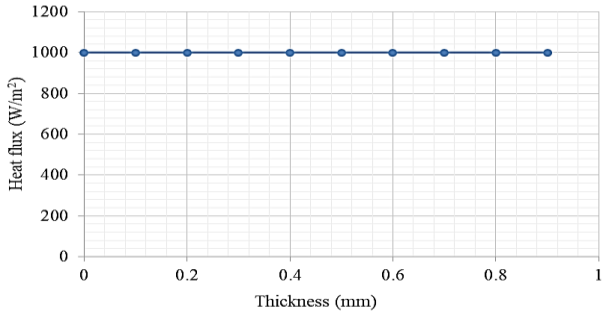

Fig. 12. Heat flux 1000 W/m^2 passed through both the systems along the thickness.

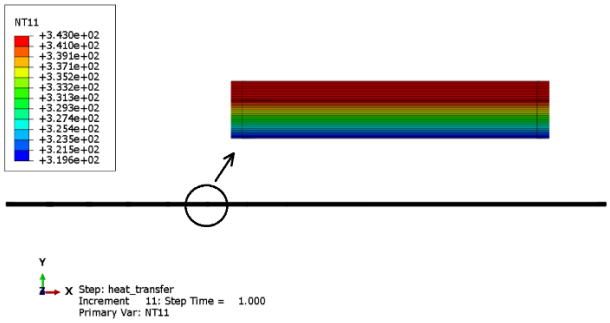

Fig. 13. Variation of nodal temperature through silicon and insulator plates.

It was found that the highest thermal conductivity of 1.9 W/mK was achieved at 20% V_f of alumina in the epoxy bisphenol-A matrix. Therefore to increase the heat transfer, instead of the insulating plate, a composite plate made of epoxy and alumina was used. The boundary and loading conditions were kept the same as in the case of a silicon/insulated plate system. When the heat was transferred through the system of silicon/composite plate, no accumulation of heat in the system was observed. The heat was conducted easily because the temperature at the bottom surface of the composite plate was found to be very close to the temperature provided to the top surface of the upper plate as shown in **Fig. 14**. The temperature difference was found to be nearly 1 K which was achieved because of the higher thermal conductivity of the bottom plate which was taken as a composite material made of alumina in the epoxy bisphenol-A matrix.

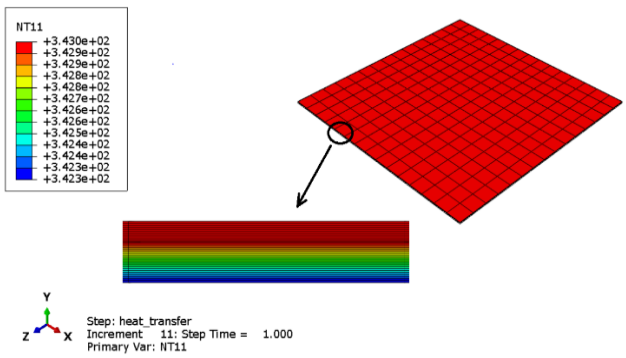

Fig. 14. Variation of temperature through the system of silicon/ composite plates along the thickness.

Conclusions

MD simulations were used for predicting the properties of epoxy (bisphenol-A) reinforced with alumina nanoparticles. The mechanical properties and thermal conductivity of the composite were predicted using BIOVIA Materials Studio. These values were then used as input while modeling a system of plates in Abaqus/Explicit. Two systems for which the heat transfer analysis was performed were: (i) Silicon and insulator plates and (ii) Silicon and composite (epoxy and alumina) plates. For performing the heat transfer analysis, both heat flux and temperature of the upper plate (silicon plate) were defined using Abaqus/Explicit. The following conclusions could be drawn from the study.

(i) Composites having V_f =15%, 20%, 21% and 25% in epoxy gave thermal conductivities of 1.63, 1.90, 1.5 and 0.77 W/mK respectively. It was found that the thermal conductivity first increased till V_f =20% and then decreased.

(ii) Young's moduli of the epoxy-alumina composite at V_f = 20% were 17.77, 5.56, and 7.06 GPa at applied stress of 50, 60, and 70 GPa respectively.

(iii) In the silicon/insulator plate system, there was found to be an accumulation of heat resulting in a decrease in temperature on the bottom surface of the insulator plate. Thus, more time was taken for the heat to conduct through this system. Whereas, when the heat was transferred through the system of silicon/ composite plate, no accumulation of heat in the system was observed. The heat was conducted easily because the temperature at the bottom surface of the composite plate was found to be very close to the temperature provided to the top surface of the upper plate.

(iv) The composite obtained by ceramics (alumina) and polymer (Epoxy) was found to be a good thermal conductor. It not only showed high thermal conductivity but it could also act as an electric insulator because ceramics are thermally conductive but electrically insulated similar to polymers.

The results of this study could be used by the electronics industry and also by industries indulged in making solar panels. The demand for materials having high thermal conductivity as well as high electrical resistivity has been increasing at a very rapid rate. This study could motivate the researchers working in the area of thermal management to develop next-generation integrated circuits, nanoelectronics, and solar panels.

Data availability

The raw/processed data required to reproduce these findings cannot be shared at this time due to legal or ethical reasons.

Acknowledgement

The authors are highly thankful to the Department of Mechanical Engineering of IIT Ropar for providing the facilities for this research.

Keywords

Abaqus, alumina, epoxy, molecular dynamics, thermal conductivity.

Received: 25 April 2020
Revised: 14 July 2020
Accepted: 17 July 2020

References

1. ABAQUS Inc Manual, Abaqus User, Abaqus Theory Guide. Version 2017, Dassault Systèmes Simulia Corp, USA, **2017**.
2. Aghdam, M.K.H.; Ansari, R.; *Compos. Part B-Eng.*, **2019**, *162*, 167.
3. Bagchi, A.; Nomura, S.; *Compos. Sci. Technol.*, **2006**, *66*, 1703.
4. Chen, H.; Ginzburg, V.V.; Yang, J.; Yang, Y.; Liu, W.; Huang, Y.; Du, L.; Chen, B.; *Prog. Polym. Sci.*, **2016**, *59*, 41.
5. Dassault Systemes BIOVIA, Materials Studio, 7.0, Dassault Systemes, San Diego, 2017.
6. Duan, Y.; Zhou, W.; Qin, J.; Bao, W.; Yu, D.; *J. Enhanc. Heat Transf.*, **2011**, *18*, 71.
7. Fu, Q.; Zhang, X.; Wu, K.; Liu, Y.; Yu, B.; Zhang, Q.; *Compos. Sci. Technol.*, **2019**, *175*, 135.
8. Han, Z.; Fina, A.; *Prog. Polym. Sci.*, **2011**, *36*, 914.
9. Jamali, J.; Aghdam, M.K.H.; Mahmoodi, M.J.; *Int. J. Heat Mass Tran.*, **2018**, *124*, 190.
10. Jouyandeh, M.; Jazani, O.M.; Navarchian, A.H.; Saeb, M. R.; *J. Reinf. Plast. Comp.*, **2016**, *35*, 1685.
11. Khelifa, A.; Touafek, K.; Moussa, H.B.; Tabet, I.; *Solar Energy*, **2016**, *135*, 169.
12. Kozako, M.; Okazaki, Y.; Hikita, M.; Tanaka, T.; Preparation and Evaluation of Epoxy Composite Insulating Materials Toward High Thermal Conductivity, In 10th IEEE Int. Conf. on Sol. Diel., Potsdam, **2010**, pp. 1-4.
13. Lei, C.; Xu, R.; Chen, M.; Zhang, F.; Huang, X.; Luo, X.; Lu, S.; Zhang, X.; *Compos. Sci. Technol.*, **2016**, *133*, 111.
14. Lin, Z.; Mcnamara, A.; Liu, Y.; Moon, K.S.; Wong, C.P.; *Compos. Sci. Technol.*, **2014**, *90*, 123.
15. Mahmoodi, M.J.; Aghdam, M.K.H.; Ansari, R.; *Int. J. Mech. Mater. Des.*, **2019**, *15*, 539.
16. Mahmoodi, M.J.; Aghdam, M.K.H.; *Mat. Sci. Eng. B.*, **2018**, *229*, 173.
17. Mai, V.D.; Lee, D.; Park, J.H.; Lee, D.S.; *Polymers*, **2019**, *11*, 597.
18. Nakayama, T.; Cho, H.B.; Suematsu, H.; Suzuki, T.; Jiang, W.; Niihara, K.; Song, E.; Eom, N.S.A.; Kim, S.; Choa, Y.H.; *Compos. Sci. Technol.*, **2016**, *129*, 205.
19. Saeb, M.R.; Karami, Z.; Jazani, O.M.; Navarchian, A.H.; *Prog. Org. Coat.*, **2018**, *125*, 222.
20. Saeb, M.R.; Najafi, F.; Ehsan Bakhshandeh, E.; Khonakdar, H.A.; Mostafaiyan, M.; Simon, F.; Scheffler, C.; Mäder, E.; *Chem. Eng. J.*, **2015**, *259*, 117.
21. Schulte, K.; Gojny, F.H.; Nastalczyk, J.; Roslaniec, Z.; *Chem. Phys Lett.*, **2003**, *370*, 820.
22. Sharma, S.; Kumar, P.; Chandra, R.; *J. Compos. Mater.*, **2017**, *51*, 3299.
23. Sharma, S.; Molecular Dynamics Simulation of NanoComposites Using Biovia Materials Studio, LAMMPS and Gromacs, Elsevier, The Boulevard, Langford Lane, Kidlington, Oxford OX5 1GB, United Kingdom, **2019**, pp. 262-296.
24. Sun, H.; *J. Phys. Chem. A*, **1998**, *5647*, 7338.
25. Tyagi, V.V.; Kaushik, S.C.; Tyagi, S.K.; *Renew. Sustain. Energy Rev.*, **2012**, *16*, 1383.
26. Xu, Y.; Chung, D.D.L.; Mroz, C.; *Compos. Pt. A Appl. Sci. Manuf.*, **2001**, *32*, 1749.
27. Xu, Z.; Li, X.; Niu, C.; Wang, Q.W.; Ma, T.; *J. Enhanc. Heat Transf.*, **2020**, *27*, 71.
28. Yang, W.; Feng, C.P.; Wan, S.S.; Wu, W.C.; Bai, L.; Bao, R.Y.; Liu, Z.Y.; Yang, M.B.; Chen, J.; *Compos. Sci. Technol.*, **2018**, *167*, 456.
29. Yilmazoglu, M.Z.; Gokalp, O.; Biyikoglu, A.; *J. Enhanc. Heat Transf.*, **2019**, *26*, 1.
30. Yu, S.; Yang, S.; Cho, M.; *Polymer*, **2009**, *50*, 945.